

Radiation effects in Low Gain Avalanche Detectors after hadron irradiations

To cite this article: G. Kramberger *et al* 2015 *JINST* **10** P07006

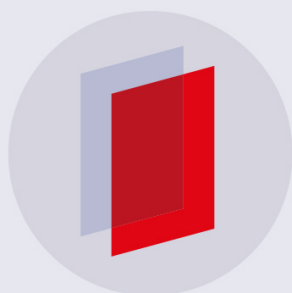
View the [article online](#) for updates and enhancements.

Related content

- [Simulation of Low Gain Avalanche Detector characteristics based on the concept of negative feedback in irradiated silicon detectors with carrier impact ionization](#)
E. Verbitskaya, V Eremin, A. Zabrodskii *et al*.
- [Technology developments and first measurements on inverse Low Gain Avalanche Detector \(iLGAD\) for high energy physics applications](#)
M. Carulla, M. Fernández-García, P. Fernández-Martínez *et al*.
- [Dependence of charge multiplication on different design parameters of LGAD devices](#)
G. Jain, R. Dalal, A. Bhardwaj *et al*.

Recent citations

- [Radiation resistant LGAD design](#)
M. Ferrero *et al*
- [Comparison of 35 and 50m thin HPK UFSD after neutron irradiation up to \$6 \cdot 10^{15}\$ neq/cm²](#)
Y. Zhao *et al*
- [Charge collection in irradiated HV-CMOS detectors](#)
B. Hiti *et al*



IOP | ebooks™

Bringing you innovative digital publishing with leading voices to create your essential collection of books in STEM research.

Start exploring the collection - download the first chapter of every title for free.

Radiation effects in Low Gain Avalanche Detectors after hadron irradiations¹

G. Kramberger,^{a,2} M. Baselga,^b V. Cindro,^a P. Fernandez-Martinez,^b D. Flores,^b Z. Galloway,^c A. Gorišek,^a V. Greco,^b S. Hidalgo,^b V. Fadeyev,^c I. Mandić,^a M. Mikuž,^{a,d} D. Quirion,^b G. Pellegrini,^b H.F-W. Sadrozinski,^c A. Studen^a and M. Zavrtanik^a

^aJožef Stefan Institute,

Jamova 39, SI-1000 Ljubljana, Slovenia

^bIMB-CNM-CSIC,

Barcelona 08193, Spain

^cUCSC, Santa Cruz Institute for Particle Physics,

Santa Cruz, CA 95064, U.S.A.

^dUniversity of Ljubljana, Faculty of Mathematics and Physics,

Jadranska 19, SI-1000 Ljubljana, Slovenia

E-mail: Gregor.Kramberger@ijs.si

ABSTRACT: Novel silicon detectors with charge gain were designed (Low Gain Avalanche Detectors - LGAD) to be used in particle physics experiments, medical and timing applications. They are based on a $n^{++}-p^+-p$ structure where appropriate doping of multiplication layer (p^+) is needed to achieve high fields and impact ionization. Several wafers were processed with different junction parameters resulting in gains of up to 16 at high voltages. In order to study radiation hardness of LGAD, which is one of key requirements for future high energy experiments, several sets of diodes were irradiated with reactor neutrons, 192 MeV pions and 800 MeV protons to the equivalent fluences of up to $\Phi_{eq} = 10^{16} \text{ cm}^{-2}$. Transient Current Technique and charge collection measurements with LHC speed electronics were employed to characterize the detectors. It was found that the gain decreases with irradiation, which was attributed to effective acceptor removal in the multiplication layer. Other important aspects of operation of irradiated detectors such as leakage current and noise in the presence of charge multiplication were also investigated.

KEYWORDS: Solid state detectors; Charge transport and multiplication in solid media; Si microstrip and pad detectors; Radiation-hard detectors

¹Work performed in the framework of the CERN-RD50 collaboration.

²Corresponding author.

Contents

1	Introduction	1
2	Samples and experimental technique	2
3	Gain and current	3
3.1	Non-irradiated samples	3
3.2	Irradiated samples	5
4	Reasons for gain degradation	7
5	Noise in multiplication mode	10
6	Conclusions	11

1 Introduction

The upgrade of the Large Hadron Collider (HL-LHC) will require substantial radiation hardness of the innermost detectors which will be exposed to fluences of up to $1.6 \cdot 10^{16}$ fast hadrons/cm² and 10 MGy of ionizing dose [1]. Although it was proven in recent years that a combination of readout at segmented n⁺ electrodes, high voltage operation, carefully planned annealing scenario and proper electrode design, both for planar and 3D detectors, leads to efficient operation of silicon detectors over the whole fluence range [2–6], the degradation of charge collection efficiency still remains the main obstacle, particularly if the applied voltages are limited to a few 100 V.

A way to overcome this difficulty is to implement a detector design where impact ionization is exploited to achieve charge gain already before irradiation. Charge gain would therefore partially

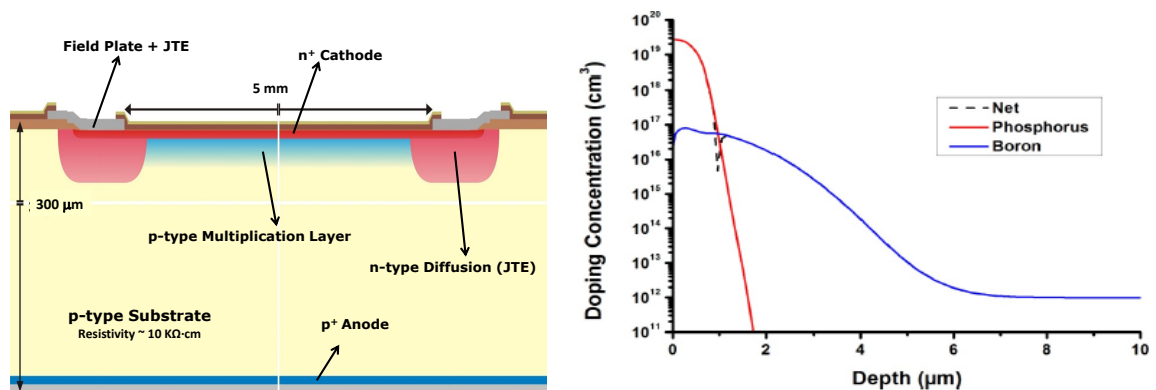


Figure 1. (a) Schematic view of devices used in the study. (b) Simulated doping profile at the n⁺⁺–p⁺ junction in the center of the investigated devices (taken from ref. [7]).

compensate for the decrease of collected charge due to trapping and reduction of the active region (increase of effective doping concentration in the bulk) with irradiation. Several wafers of sensors were fabricated (see figure 1) where a highly doped p-layer was implanted under the n^{++} well to reach the required electric field strengths [7]. The design is similar to the one of the Avalanche Photo Diodes, but with proper electrode isolation techniques, it allows also for production of segmented sensors.

The aim of this work is to determine the effect of radiation on the performance of Low Gain Avalanche Detectors (LGAD). Apart from the dependence of the gain on the fluence and type of radiation, the leakage current and noise performance are also investigated.

2 Samples and experimental technique

The investigated LGAD were 300 μm thick pad detectors with sensitive area of $5 \times 5 \text{ mm}^2$ (figure 1) processed on Float zone p-type silicon ($\sim 10 \text{ k}\Omega\text{cm}$). They had an opening in metallization at the junction side to allow for visible light illumination. The metallization on the back side was partly etched away after processing for the same purpose. The measured gain ranged between 2 and 16, depending on the multiplication layer properties and applied bias voltage as will be shown in the next section.

The samples were irradiated with neutrons at Jožef Stefan Institute research reactor [8], with 800 MeV protons at Los Alamos National Laboratory and 192 MeV pions at Paul Scherrer Institute in Villigen, Switzerland [9]. They were characterized by Transient Current Technique (TCT) [10] and charge collection measurement with electrons from ^{90}Sr source with LHC speed electronics (CCE). The experimental setups are shown in figure 2. The detailed description of the setups can be found in [11] for the TCT and [12] for the CCE. In the latter the source is collimated to the extent that the almost all electrons ($> 97\%$) that reach the scintillator and trigger the readout have crossed the detector, thus allowing the measurements of the signal even at very low signal-to-noise ratios.

The measurements were performed after annealing for 80 min at 60°C . Some of the neutron irradiated samples were irradiated in several steps with annealing procedure done after each step (CERN scenario [13]). The fluences of particles were scaled to 1 MeV neutron equivalent fluences by using hardness factors: 0.92 for reactor neutrons ($> 100 \text{ keV}$) [14], 1.14 for 192 MeV pions [13] and 0.71 for 800 MeV protons [15]. The uncertainty of delivered fluences is 10% for neutrons and 8% for charged hadrons.

The samples originated from two different wafers, hereafter referred to as W7 and W8. They differed in the implantation dose of Boron: $1.6 \cdot 10^{13} \text{ ions cm}^{-2}$ for W7 and $2 \cdot 10^{13} \text{ ions cm}^{-2}$ for W8 (resulting doping profile shown in figure 1b).

Examples of deposited energy spectra of ^{90}Sr electrons for a LGAD and a standard Float Zone p-type pad detector ($V_{fd} \sim 80 \text{ V}$) are shown in figure 3a. A much larger signal corresponding to most probable energy loss (peaks in spectra) in LGAD can be observed. The reason for such a behaviour can be seen in figure 3b, which shows time dependence of induced current measured with TCT setup after short laser pulses of red light directed to the back side of the LGAD from W8. Different stages of signal formation can be identified: injection of electrons, drift of electrons, onset of multiplication at $n^{++}\text{-p}^+$ junction and consequent drift of multiplied

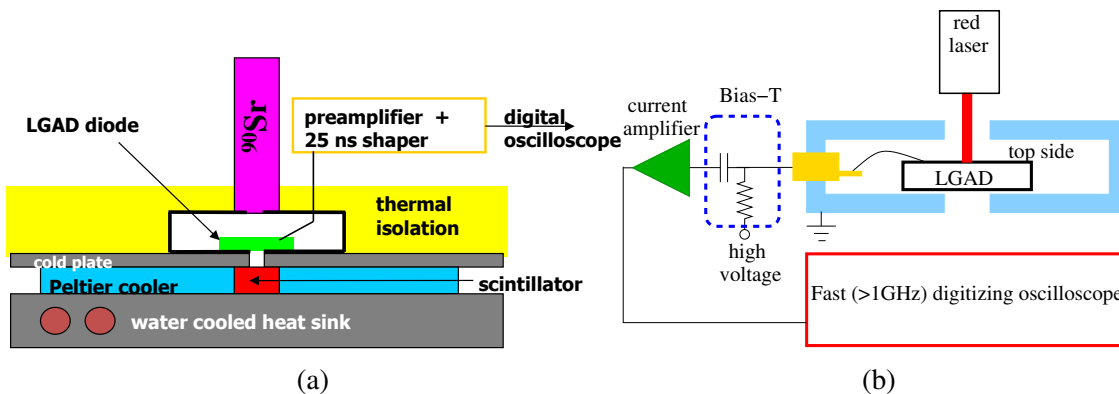


Figure 2. Schematic view of the experimental setup for: (a) charge collection measurements and (b) for TCT measurements (350 ps pulse, $\lambda = 660$ nm, 200 Hz repetition).

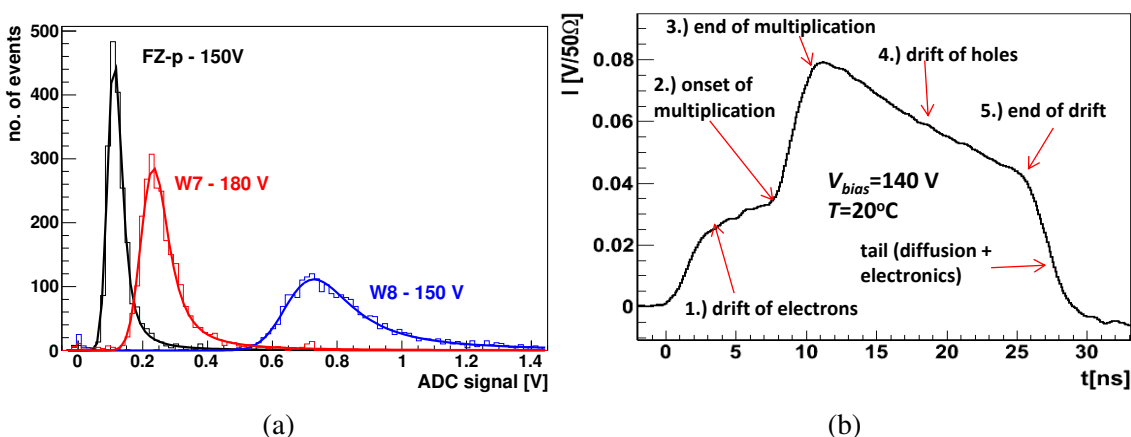


Figure 3. Comparison of the energy loss spectra of minimum ionizing electrons from ^{90}Sr obtained with the LGAD and the standard Float Zone p-type pad detector of the same thickness. Fits of Landau function convoluted with Gaussian to the spectra are also shown. (b) Measured induced current in a W8 sample with indicated stages of signal evolution after illumination of the detector’s back side by a short pulse of red light.

holes. A large amplification is evident from comparison of the induced currents before and after multiplication.

3 Gain and current

3.1 Non-irradiated samples

A set of several samples from both wafers were investigated before irradiation. A very good gain homogeneity was observed across the wafer showing a good control of the doping profile (see figures 4a,b). The dependence of collected charge on voltage has a very distinct shape. Almost no charge is measured up to around 30 V which is the voltage required to deplete the multiplication p^+ layer (V_{mr}). Electric field in the multiplication layer becomes high enough for charge multiplication and at larger bias voltages the charge rises steeply as the bulk of the device is depleting thus generating additional electrons available for multiplication. After bulk depletion, the charge rises

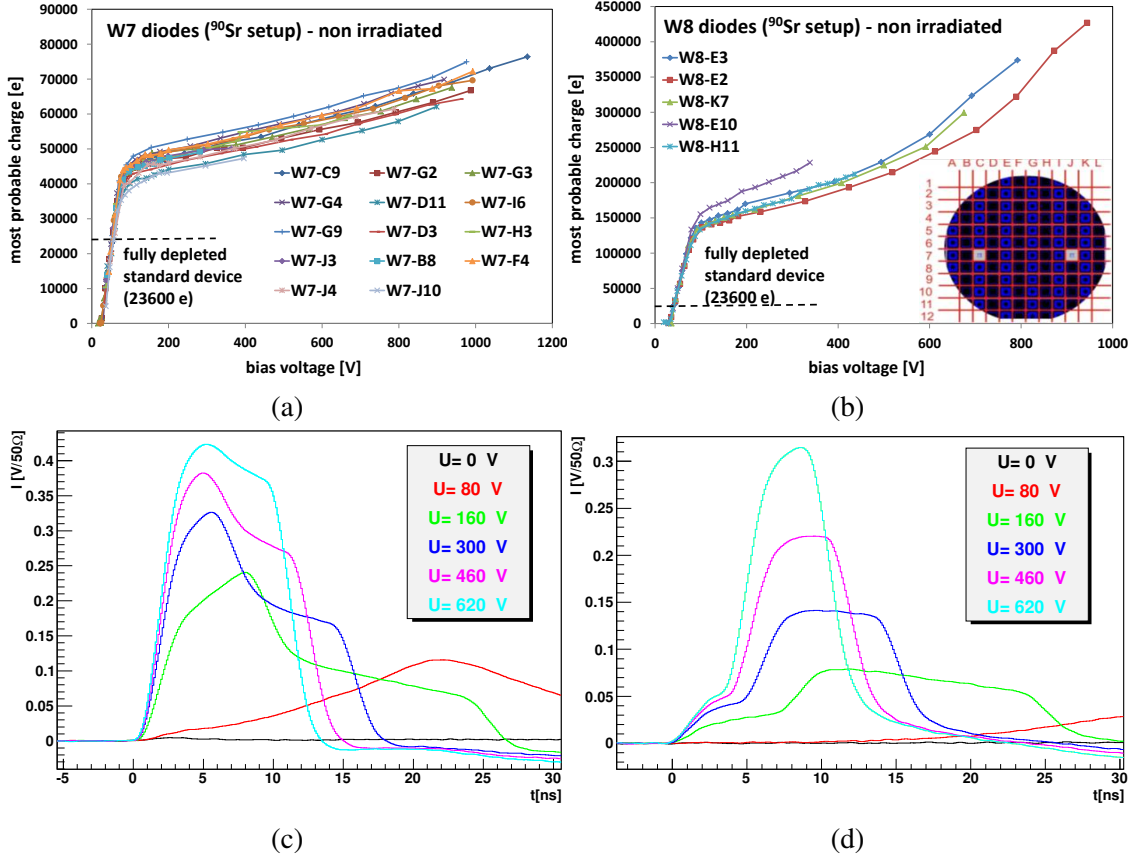


Figure 4. Dependence of measured charge on bias voltage at $T = -10^\circ\text{C}$ for different non-irradiated samples across wafers (a) W7 and (b) W8. The dashed line denotes the charge in fully depleted standard detector of the same thickness. The inset in (b) shows the location of the sensors in the wafers. Induced currents (TCT) in the detectors from (c) W7 and (d) W8 after detector back illumination (electron injection).

moderately as any additional applied voltage drops equally over the entire thickness, hence 300 V is required to raise the electric field by $1\text{ V}/\mu\text{m}$ in the multiplication layer.

The TCT signals after back side illumination (electron injection) are shown in figures 4c,d. A clear difference between LGAD from W7 and W8 can be observed in the gain. After the multiplication the hole current is somewhat smaller for W7 and substantially larger for W8 than the electron current before multiplication. Note that charge collection time in LGAD is larger than for standard detectors due to additional drift times of multiplied holes.

Unlike gain, the leakage current of devices varied for almost three orders of magnitude between the samples across the wafer with no obvious systematic trend (see. figures 5a,b). The origin of the high current is not clear to us. It does not scale with temperature as expected for the generation current, but exhibits rather weak temperature dependence as shown in figure 5c.

The devices with high excess current exhibit positive space charge in the bulk after neutron irradiations already before the onset of multiplication (details in ref. [16]). This leads to a conclusion that a larger part of the excess current is related to hole injection in the bulk somewhere at the $n^{++}\text{-}p^+$ contact. Trapped holes at radiation induced deep energy levels change the space charge from negative, as usually observed in neutron irradiated detectors, to positive. Modification

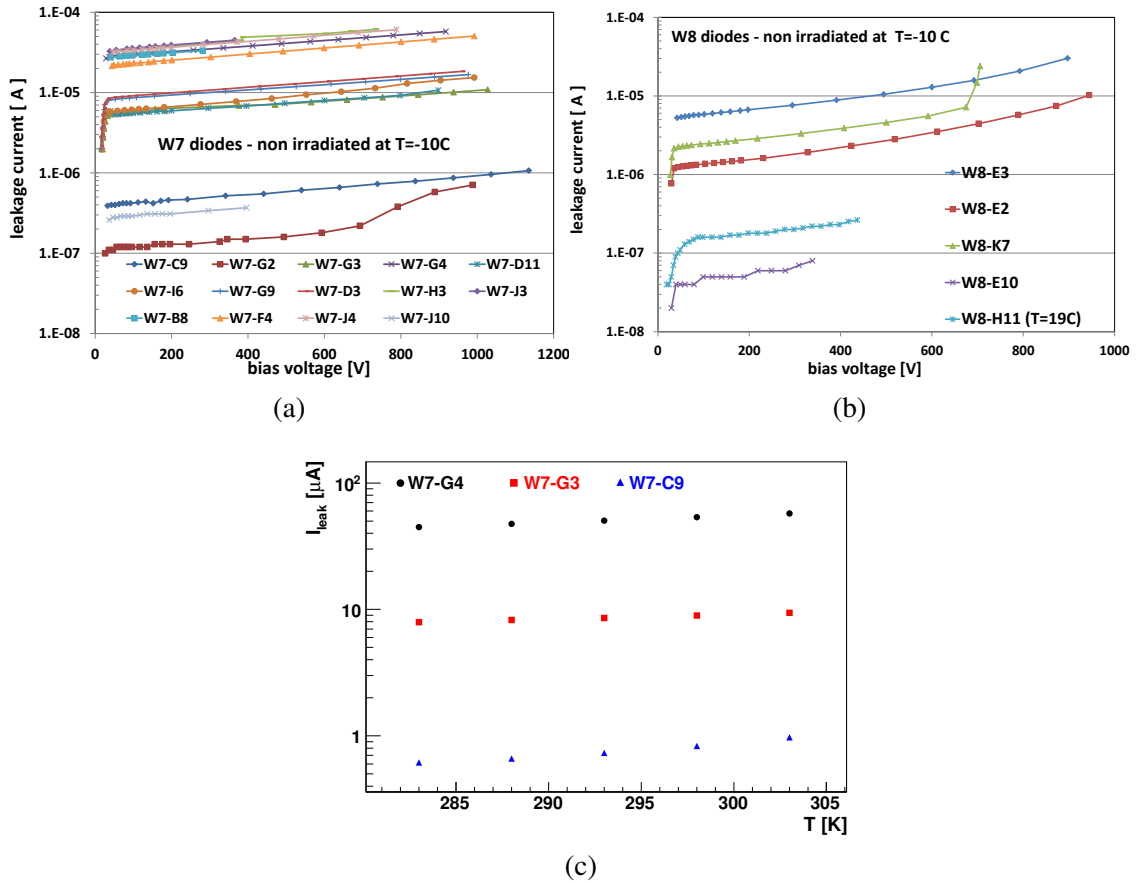


Figure 5. Leakage current dependence on voltage at $T = -10^\circ\text{C}$ for LGAD: (a) from W7 and (b) W8. (c) Dependence of leakage current on temperature at 400 V for different samples.

of space charge in irradiated detectors by excess carriers leads to complicated interpretation of the results, therefore for the radiation damage studies only the samples with small current ($< \text{few } \mu\text{A}$ at 20°C) were selected.

3.2 Irradiated samples

The dependence of charge collection on fluence is shown in figure 6. Samples from both wafers were irradiated with neutrons. Selected samples from W8 were irradiated with 800 MeV protons and those from W7 with 192 MeV pions. It can clearly be seen that at already moderate fluences the measured charge rapidly decreases. The decrease is larger for charged hadrons irradiated samples than for reactor neutrons. Already at fluences of few 10^{14} cm^{-2} the gain almost completely vanishes for charged hadrons irradiated samples as can be seen in figure 6d where the LGAD is compared to a control pad detector without p^+ layer (denoted by W9) irradiated together.

The dependence of measured charge at 500 V and 1000 V on equivalent fluence is shown in figure 7 and compared to the standard Float Zone p-type pad detectors processed by Micron with same dimensions and similar initial resistivity [17]. It seems that for neutron irradiated samples the gain, defined as $M_Q = Q_{LGAD}/Q_{std}$, has not completely vanished at $\Phi_{eq} \sim 2 \cdot 10^{15} \text{ cm}^{-2}$, but

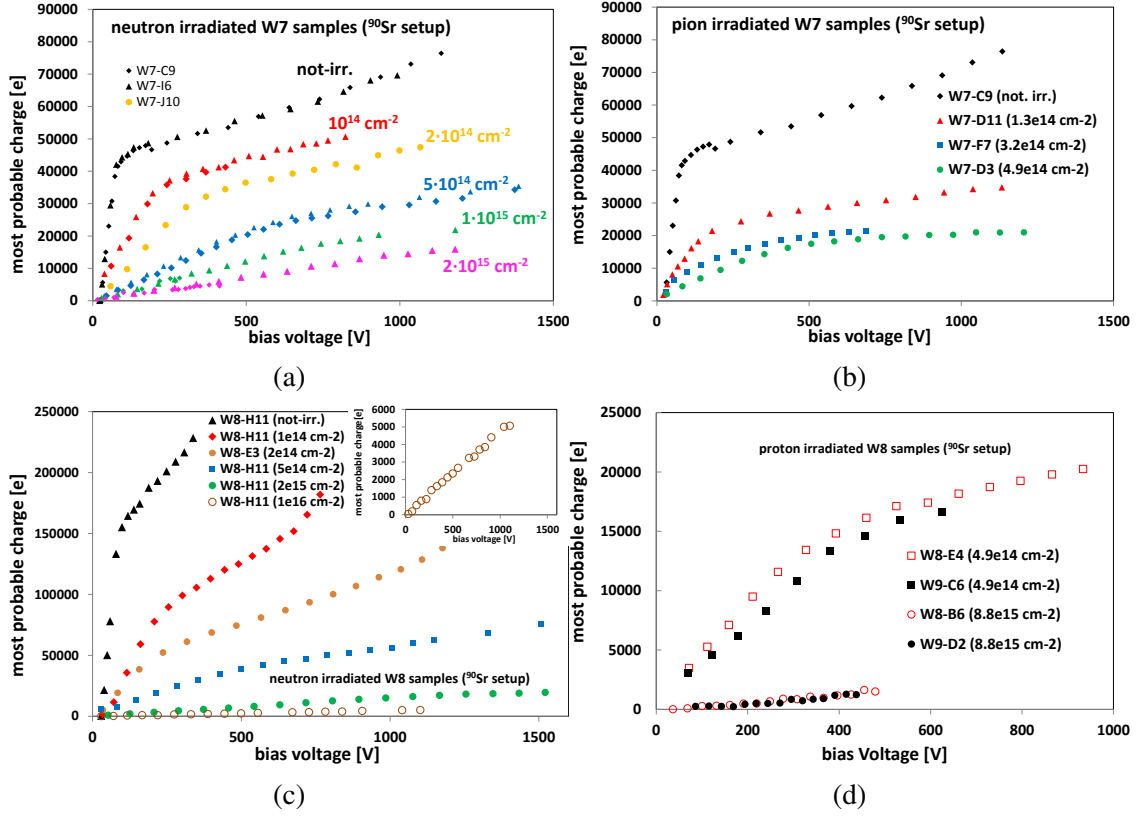


Figure 6. Dependence of most probable charge on voltage at different equivalent fluences for (a) neutron irradiated LGAD from W7 (b) 192 MeV pion irradiated LGAD from W7 (c) neutron irradiated LGAD from W8 (irradiated in steps) and (d) 800 MeV proton irradiated LGAD from W8 and a standard control diode from W9. The measurements were done at $T = -10^\circ\text{C}$ for (a,b,d) and at $T = -20^\circ\text{C}$ for (d). The samples were annealed for 80 min at 60°C prior to the measurements.

there is little difference between devices from both wafers. On the other hand, the loss of gain for charged hadron irradiated devices is almost complete at $\Phi_{eq} \sim 5 \cdot 10^{14} \text{ cm}^{-2}$.

The leakage current of irradiated LGAD follows the relation

$$I = M_I I_{gen} = M_I(\Phi_{eq}) \alpha \Phi_{eq} V \quad , \quad (3.1)$$

where I_{gen} is the generation current, α leakage current damage constant [18], V active volume of the detector and M_I current multiplication factor. In general $M_I \geq M_Q$ as the trapped carriers get eventually detrapped thus contributing to the current, but not to the charge measured in 25 ns.

The relative increase of I_{leak} with fluence in LGAD is therefore smaller than for standard detectors (see figures 8). The current multiplication factor can be measured at each fluence as the ratio of measured and calculated generation current (see eq. (3.1)). For more reliable determination the current can be measured at different temperatures exploiting the fact that M_I is weakly dependent on temperature compared to the generation current. An example of such determination is seen in figures 9, where the M_I is obtained as the slope of I_{leak} vs. I_{gen} dependence.

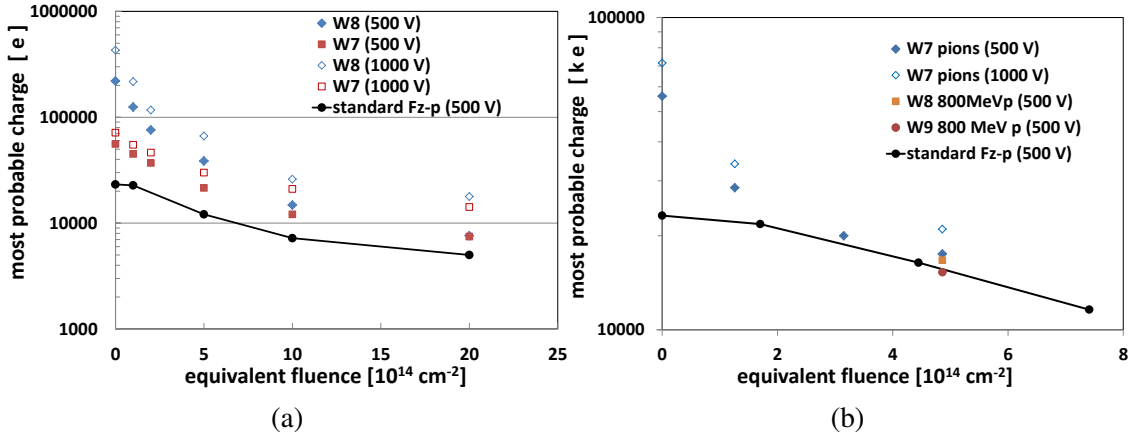


Figure 7. Dependence of measured charge on equivalent fluence at 500 V and 1000 V for (a) neutron irradiated LGAD and (b) charged hadrons irradiated LGAD. Measured charge in a standard diode at 500 V is also shown for the reference [17].

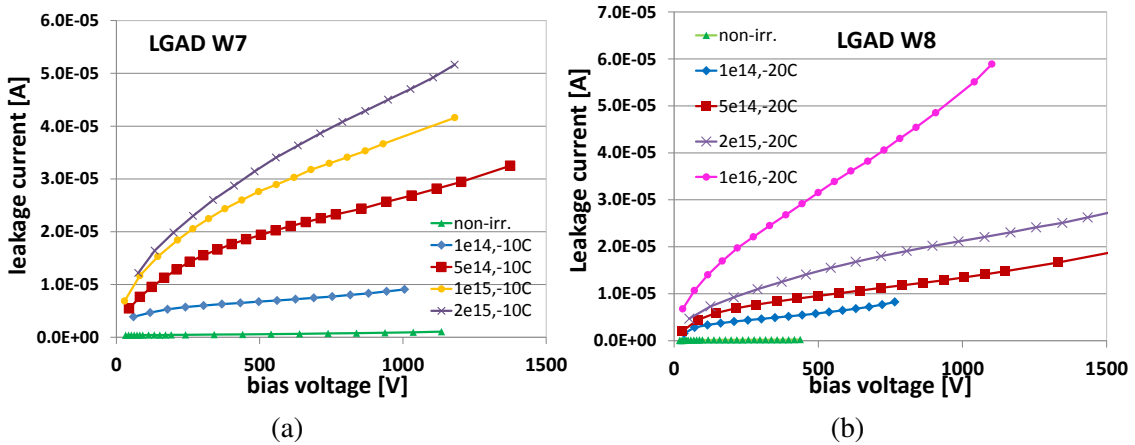


Figure 8. Leakage current dependence on fluence for low excess current samples from (a) W7 and (b) W8.

4 Reasons for gain degradation

The relative decrease of measured charge is much more pronounced for LGAD than for standard devices at fluences below 10^{15} cm^{-2} [17] (see figure 7). The reason must therefore be related to the decrease of the multiplication gain rather than trapping of the drifting charge. This reasoning is confirmed by comparing induced currents in irradiated LGAD from W7 and W8 after back side illumination (see figures 10a,b) with those before irradiation (see figures 4c,d). A significant decrease of the induced current after multiplication with respect to the induced current before its onset is evident at all applied voltages.

The gain decrease can be attributed to the reduction of effective doping in multiplication layer, which leads to smaller electric field strengths. The voltage required to deplete the p^+ layer, can be probed by the TCT with front illumination of the detector by light of short penetration depth. The induced current is only observed once the p^+ layer is depleted, followed by depletion region growth in the p bulk at larger bias voltages. Only when the carriers drift over a significant distance

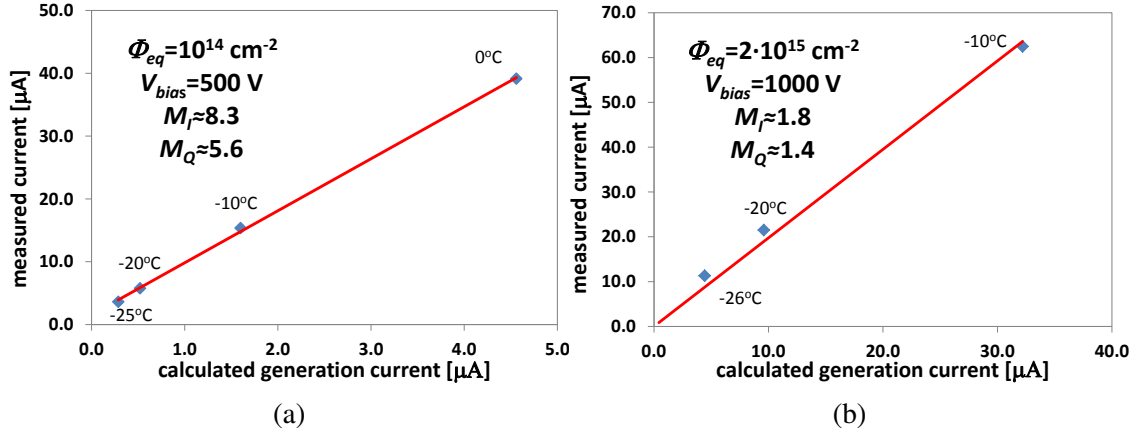


Figure 9. Comparison of measured and calculated generation current at different temperatures for a W8 sample irradiated to (a) $\Phi_{eq} = 10^{14} \text{ cm}^{-2}$ and (b) $\Phi_{eq} = 2 \cdot 10^{15} \text{ cm}^{-2}$. The slope of the line (red) denotes the current amplification. Approximate values of corresponding M_Q are also given.

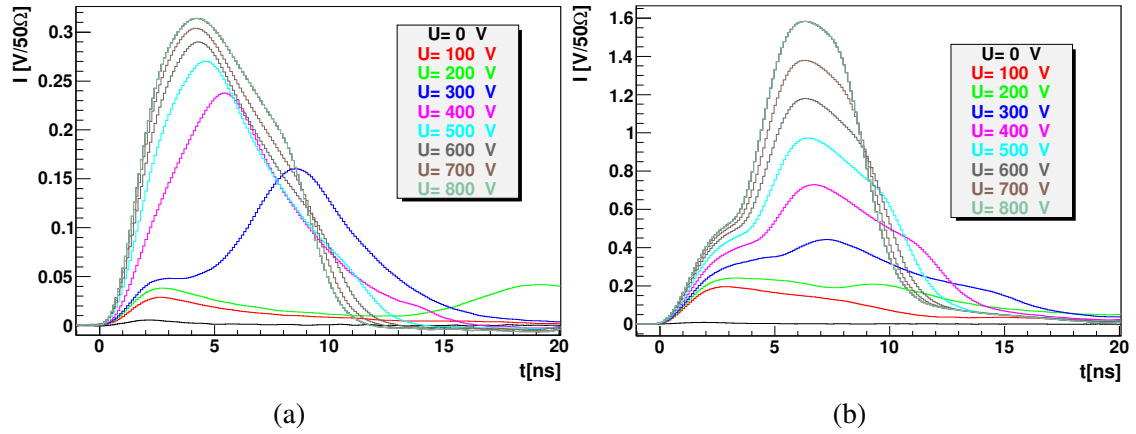


Figure 10. Measured induced currents after back illumination in the LGAD irradiated to $\Phi_{eq} = 2 \cdot 10^{14} \text{ cm}^{-2}$ from (a) W7 and (b) W8.

without recombination the current is induced as shown in the inset of figure 11a. In figures 11 the integral of the current in 20 ns can be observed for samples from W7 irradiated with neutrons and pions.

Values of V_{mr} were obtained by fitting $Q \propto \sqrt{V_{bias} - V_{mr}}$ to the measured curves. It can be clearly seen that V_{mr} decreases with equivalent fluence, faster for pions than reactor neutrons. This is in agreement with gain degradation after charged hadron and neutron irradiations. If it is assumed that the removal of effective acceptors (N_A) occurs with the same rate everywhere in the p^+ layer, then the V_{mr} is proportional to an average N_A in the p^+ layer. Decrease of N_A can be a consequence of initial boron removal or compensation of effective acceptors by holes produced in multiplication and trapped at the energy levels in the band-gap. The dependence of V_{mr} on equivalent fluence is shown in figure 12. The initial acceptor removal is exponentially dependent on fluence

$$N_A = N_{A,0} \exp(-c \Phi_{eq}) \quad \Rightarrow \quad V_{mr} \approx V_{mr,0} \exp(-c \Phi_{eq}) \quad , \quad (4.1)$$

where c is the removal constant $N_{A,0}$ initial doping concentration and $V_{mr,0}$ corresponding multi-

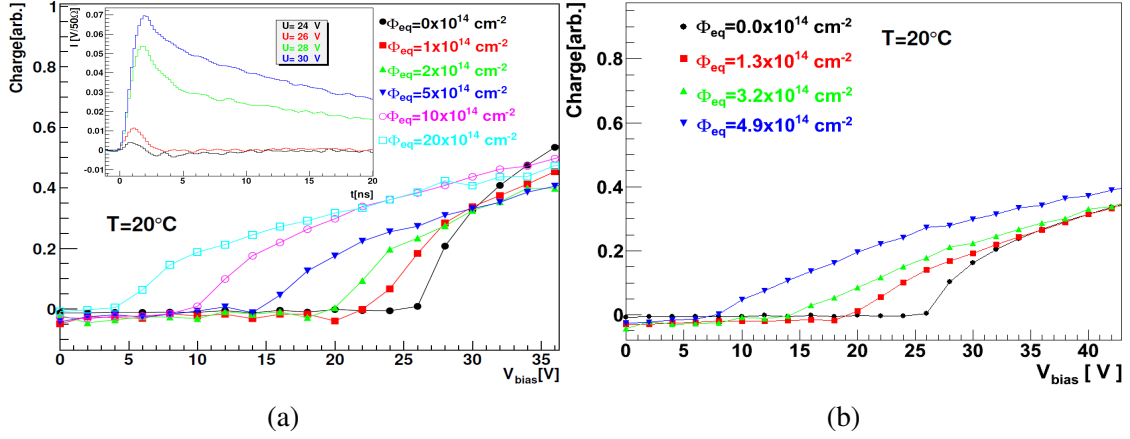


Figure 11. (a) Dependence of measured charge in 20 ns on bias voltage after front illumination of the LGAD from W7 irradiated to different fluences for: (a) reactor neutrons and (b) 192 MeV pions. Examples of induced current in non-irradiated detector are shown in the inset of (a).

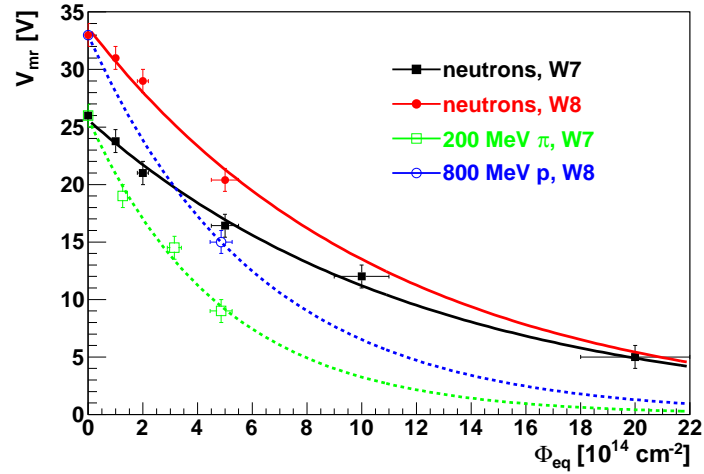


Figure 12. Dependence of V_{mr} on the equivalent fluence. The fit of eq. (4.1) to the measured points is also shown.

plication layer depletion voltage. The investigated fluence range for the neutron irradiated LGAD from W7 was large enough to confirm that the decrease of N_A is due to boron removal, i.e. follows eq. (4.1). A space charge compensation due to trapped holes would result in a linear decrease of N_A provided that first order reactions are responsible. The values of removal constant were found to be: $c_{W8,p} \approx 16 \cdot 10^{-16} \text{ cm}^{-2}$, $c_{W8,n} \approx 9.1 \cdot 10^{-16} \text{ cm}^{-2}$, $c_{W7,\pi} \approx 20 \cdot 10^{-16} \text{ cm}^{-2}$ and $c_{W7,n} = 8.2 \cdot 10^{-16} \text{ cm}^{-2}$. The uncertainties of the removal constants derived from the fits were between 10% ($c_{W7,n}$) and 20% ($c_{W8,p}$) with an estimation that V_{mr} were determined with precision of $< 1 \text{ V}$.

The removal constants are much smaller than measured in high resistivity silicon [19]. A good agreement between removal constant for both wafers points to the conclusion that in the given doping range the removal constant does not exhibit strong dependence on concentration.

The faster removal of effective acceptors for charged hadrons may be related to the defect

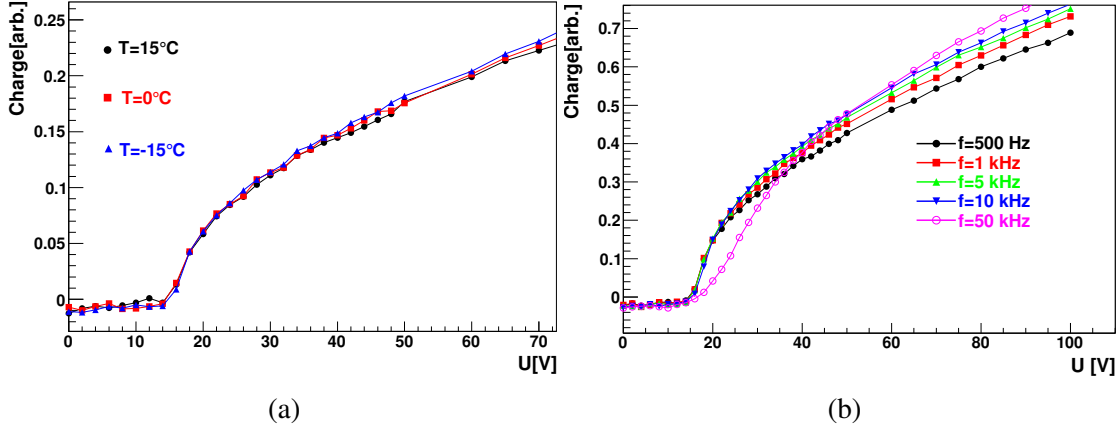


Figure 13. (a) Induced charge after front illumination of the LGAD from W7 at: (a) different temperatures and (b) different laser frequencies at $T = 20^\circ\text{C}$, showing no effect on V_{mr} .

kinetics. Charged hadrons produce larger fraction of point defects at a given non-ionizing energy loss. These are more homogeneously distributed over the volume therefore exhibiting large probability for reaction with boron atoms [20]. A way to improve the radiation hardness would be doping of p^+ layer with Gallium [21], which is more difficult to displace.

Another strong argument that initial acceptor removal is responsible for lower gain is the dependence of V_{mr} on temperature and free carrier concentration. In case of compensation the occupation probability of traps would depend on temperature and also on free carrier concentration. As shown in figure 13a, V_{mr} is insensitive to temperature change in the range -15°C to 15°C . Also the change of laser pulse frequency, which influences the amount of trapped charges in the multiplication layer, showed no effect on V_{mr} (see figure 13b).

5 Noise in multiplication mode

The use of LGAD detectors requires a careful optimization as the increase of noise due to multiplication can diminish the benefits or even deteriorate the performance. The noise equivalent charge (in units of elementary charge, e_0) for a readout scheme where the electrode is connected to a charge sensitive preamplifier (integrator) followed by a pulse shaping circuitry is usually given by the sum of series and parallel noise $ENC^2 = ENC_s^2 + ENC_p^2$. Series noise (i.e. voltage noise) ENC_s depends mainly on capacitance of the electrode, shaping time τ and the design of the amplifier [22, 23]. It was in our case $ENC_s = 2700 e_0$ for the LGAD from W8 and $\tau = 25$ ns. The parallel noise ENC_p , is in the case of the LGAD, dominated by the shot (current) noise and can be written as [22–24]

$$ENC_p = k_f M_I \sqrt{F} \sqrt{e_0 I_{gen} \tau} \quad (5.1)$$

where F is noise excess factor [24, 25] and k_f is a constant depending on the type of pulse shaping. Precise value of k_f is not known to us, therefore $k_f = 1$ was assumed which gives a good agreement and is close to that for a simple CR-RC pulse shaping ($k_f = 1.35$). The calculated noise was compared to the measured noise for the LGAD from W8 at $\Phi_{eq} = 10^{14} \text{ cm}^{-2}$ and $\Phi_{eq} = 2 \cdot 10^{15} \text{ cm}^{-2}$ (see figure 14). In order to minimize the effect due to different gain, electric field or trapping,

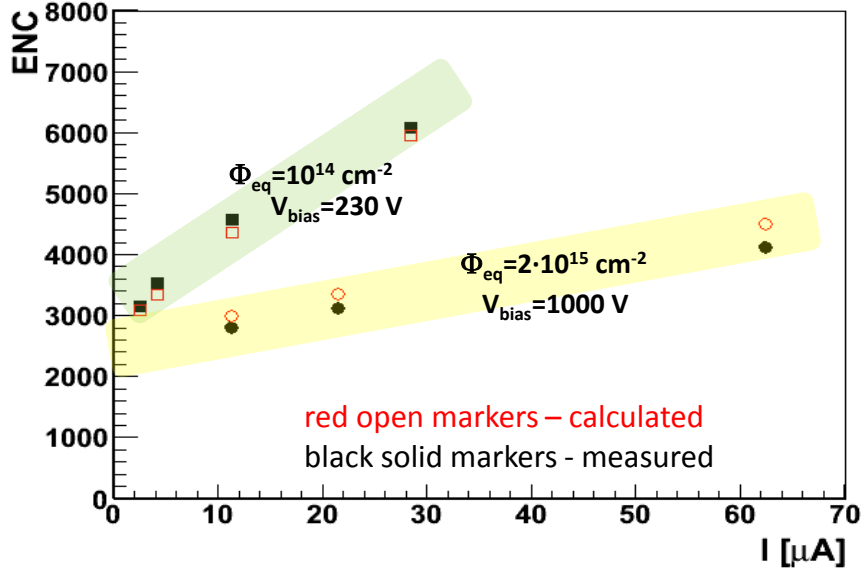


Figure 14. Comparison of the calculated and measured noise for the LGAD from W8 (fluence points grouped and denoted by bands). The points correspond to $T = 0, -10, -20, -25^\circ\text{C}$, with 0°C missing at high fluence due to a limitation of the experimental setup.

the current was varied by changing temperature rather than bias voltage. The latter was fixed to just above full depletion for measurements at low fluence and at 1000 V at high fluence. $F = 2$ ($M_I \gg 1$) and $F = 1$ ($M_I \sim 1$) were assumed for low and high fluence (see also figure 9), respectively. A reasonable agreement was found confirming the calculation.

The signal to noise ratio of the LGAD is given by

$$\frac{S}{N} = \frac{M_Q Q}{\sqrt{ENC_S^2 + k_f^2 F M_I^2 e_0 I_{gen} \tau}} \quad (5.2)$$

If an improvement of signal-to-noise ratio is the main reason for using LGAD, the following should hold

$$ENC_S^2 \gg k_f^2 F M_I^2 e_0 I_{gen} \tau \quad (5.3)$$

Hence, LGAD offer advantage over conventional detectors for small cell volumes and fast shaping times.

6 Conclusions

Radiation hardness of Low Gain Avalanche Detectors was studied after irradiations with reactor neutrons and charged hadrons. The gain of the devices decreased fast and almost vanished at irradiation fluences of $\sim 10^{15}$ fast hadrons cm^{-2} . The decrease of the gain after irradiation was attributed to removal of acceptors in the p^+ layer. The removal was faster for charged hadrons. The leakage current increased due to linear increase of generation current with fluence, but was moderated by the decrease of multiplication. The calculated impact of multiplication on the noise was in

reasonable agreement with measurements, which led to conclusion that LGAD would outperform standard detectors in terms of signal to noise for fast readout and small cell volumes.

Acknowledgments

The authors would like to thank M. Glaser (CERN) and Sally Seidel (UNM) for their help with pion and proton irradiations. This research has been partially financed by Spanish Ministry of Economy and Competitiveness through grants FPA2013-48387-C6-2-P and FPA2013-48308-C2-1-P

References

- [1] F. Gianotti et al., *Physics potential and experimental challenges of the LHC luminosity upgrade*, *Eur. Phys. J. C* **39** (2005) 293 [[hep-ph/0204087](#)].
- [2] J. Weingarten et al., *Planar Pixel Sensors for the ATLAS Upgrade: Beam Tests results, 2012 JINST 7 P10028* [[arXiv:1204.1266](#)].
- [3] RD50 collaboration, A. Dierlamm, *Silicon detectors for the SLHC: An overview of recent RD50 results*, *Nucl. Instrum. Meth. A* **624** (2010) 396.
- [4] RD50 collaboration, F. Hartmann, *Recent advances in the development of semiconductor detectors for very high luminosity colliders*, *Nucl. Instrum. Meth. A* **617** (2010) 543.
- [5] I. Mandic, V. Cindro, G. Kramberger and M. Mikus, *Measurement of anomalously high charge collection efficiency in $n+$ p strip detectors irradiated by up to 10^{-16} -n(eq)/cm²*, *Nucl. Instrum. Meth. A* **603** (2009) 263.
- [6] C. Da Via et al., *3D silicon sensors: Design, large area production and quality assurance for the ATLAS IBL pixel detector upgrade*, *Nucl. Instrum. Meth. A* **694** (2012) 321.
- [7] G. Pellegrini et al., *Technology developments and first measurements of Low Gain Avalanche Detectors (LGAD) for High Energy Physics applications*, *Nucl. Instrum. Meth. A* **765** (2014) 12.
- [8] L. Snoj, G. Žerovnik and A. Trkov, *Computational analysis of irradiation facilities at the JSI TRIGA reactor*, *Appl. Radiat. Isot.* **70** (2012) 483.
- [9] User guide to accelerator facilities, Paul Scherrer Institute, Villigen and Wurenlingen, 2nd Edition, July 1994.
- [10] V. Eremin, N. Strokan, E. Verbitskaya and Z. Li, *Development of transient current and charge techniques for the measurement of effective net concentration of ionized charges (N_{eff}) in the space charge region of p - n junction detectors*, *Nucl. Instrum. Meth. A* **372** (1996) 388.
- [11] G. Kramberger, V. Cindro, I. Mandic, M. Mikuz and M. Zavrtanik, *Effective trapping time of electrons and holes in different silicon materials irradiated with neutrons, protons and pions*, *Nucl. Instrum. Meth. A* **481** (2002) 297.
- [12] G. Kramberger et al., *Charge collection properties of heavily irradiated epitaxial silicon detectors*, *Nucl. Instrum. Meth. A* **554** (2005) 212.
- [13] ROSE collaboration, G. Lindström et al., *Radiation hard silicon detectors developments by the RD48 (ROSE) Collaboration*, *Nucl. Instrum. Meth. A* **466** (2001) 308.
- [14] D. Zontar, V. Cindro, G. Kramberger and M. Mikuz, *Time development and flux dependence of neutron-irradiation induced defects in silicon pad detectors*, *Nucl. Instrum. Meth. A* **426** (1999) 51.

- [15] S. Seidel et al., *Depletion Voltage and Effective Doping Concentration of Float Zone and Magnetic Czochralski Silicon Diodes Irradiated by Protons to Conditions Relevant to the High Luminosity LHC*, Presented at 19th RD50 Workshop, CERN, Geneva, 21-23.11.2011.
- [16] G.Kramberger et al., *Effects of irradiation on LGAD devices with high excess current*, Presented at 25th RD50 Workshop, CERN, Geneva, 17-19.11.2014
- [17] G. Kramberger et al., *Comparison of pad detectors produced on different silicon materials after irradiation with neutrons, protons and pions*, *Nucl. Instrum. Meth. A* **612** (2010) 288.
- [18] CERN-ROSE/RD48 collaboration, M. Moll, E. Fretwurst and G. Lindström, *Leakage current of hadron irradiated silicon detectors - material dependence*, *Nucl. Instrum. Meth. A* **426** (1999) 87.
- [19] R. Wunstorff et al., *Investigations of donor and acceptor removal and long term annealing in silicon with different boron/phosphorus ratios*, *Nucl. Instrum. Meth. A* **377** (1996) 228.
- [20] I. Pintiliea, G. Lindstroem, A. Junkes and E. Fretwurst, *Radiation Induced Point and Cluster-Related Defects with Strong Impact to Damage Properties of Silicon Detectors*, *Nucl. Instrum. Meth. A* **611** (2009) 52 [[arXiv:0907.3050](https://arxiv.org/abs/0907.3050)].
- [21] A. Khana et al., *Strategies for improving radiation tolerance of Si space solar cells*, *Solar Energy Mater. Solar Cell.* **75** (2003) 271.
- [22] V. Radeka, *Low noise techniques in detectors*, *Ann. Rev. Nucl.Part. Sci.* **38** (1988) 217.
- [23] H. Spieler, *Semiconductor Detector Systems*, Oxford University Press, 2005, ISBN-10:0198527845.
- [24] R.J. McIntyre, *Multiplication Noise in Uniform Avalanche Diodes*, *IEEE Trans. Electron Dev.* **ED13** (1966) 164.
- [25] P.P. Webb, R.J. McIntyre and J. Conradi, *Properties of avalanche photodiodes*, *RCA Review* 35 (1974) 234.